Case Report

A Novel Variant of the *ACTRT1* Gene is Potentially Associated with Oligoasthenoteratozoospermia, Acrosome Detachment, and Fertilization Failure

Olga Solovova *, Sabina Khayat, Sergey Bogolyubov, Elizaveta Bragina, Tatiana Cherevatova, Vyacheslav Chernykh

Posted Date: 13 November 2025

doi: 10.20944/preprints202511.1008.v1

Keywords: perinuclear theca; acrosome; TEM; spermatozoa; *ACTRT1*; oligozoospermia; teratozoospermia; male infertility; whole exome sequencing

Case Report

A Novel Variant of the *ACTRT1* Gene is Potentially Associated with Oligoasthenoteratozoospermia, Acrosome Detachment, and Fertilization Failure

Olga Solovova [1,*], Sabina Khayat [1], Sergey Bogolyubov [2,3], Elizaveta Bragina [1,4], Tatiana Cherevatova [1] and Vyacheslav Chernykh [1,5]

[1] Research Centre for Medical Genetics, 115522, Moscow, Russia
[2] Endocrinology Research Centre, 117292, Moscow, Russia
[3] Next Generation Clinic, 107140, Moscow, Russia
[4] Belozersky Institute of Physico-Chemical Biology, Lomonosov Moscow State University, 119992 Moscow, Russia
[5] Pirogov Russian National Research Medical University of the Ministry of Healthcare of the Russian Federation, 117997 Moscow, Russia
* Correspondence: olga_pilyaeva@list.ru

Abstract

Background: Male infertility is a common reproductive disorder, affecting about 7% of men in the general population. Despite its prevalence, the cause of infertility is often unknown. This case report presents the results of a comprehensive evaluation of a patient with severe oligoteratozoospermia and primary infertility. **Methods:** The patient underwent clinical, andrological, and genetic examinations, including semen analysis, transmission electron microscopy, cytogenetic examination, molecular analysis of the AZF locus and the *CFTR* gene, whole exome sequencing and Sanger sequencing. **Results:** Semen analysis revealed severe oligoasthenoteratozoospermia. Transmission electron microscopy showed acrosome detachment from the nucleus in 49% of the spermatozoa. A high percentage of spermatozoa with insufficiently condensed ("immature") chromatin (54%) was also observed. No chromosomal abnormalities, Y chromosome microdeletions, or pathogenic *CFTR* gene variants were identified. Whole exome sequencing revealed a novel c.821G>C variant (chrX:127185365G>C; NM_138289.4) in the *ACTRT1* gene (Xq25). This variant was hemizygous in the patient and heterozygous in his mother, as determined by Sanger sequencing. According to the ACMG guidelines (PM2, PP3), this missense variant in the *ACTRT1* gene was classified as a variant of uncertain clinical significance (VUS). Amino acid conservation and 3D protein modeling predict that the identified variant has a deleterious effect on the protein. **Conclusions:** This study demonstrates that hemizygous variants of the *ACTRT1* gene can cause X-linked specific teratozoospermia characterized by acrosome detachment from the sperm nucleus. These findings underscore the importance of genetic testing for infertile men with specific morphological abnormalities.

Keywords: perinuclear theca; acrosome; TEM; spermatozoa; *ACTRT1*; oligozoospermia; teratozoospermia; male infertility; whole exome sequencing

1. Introduction

Male infertility affects around 7% of men worldwide and contributes to nearly half of all infertility cases in couples [1]. Despite advances in molecular genetics, the cause of azoospermia, severe oligozoospermia, and rare syndromic forms of astheno-/teratozoospermia remains unclear for many patients [2]. Many idiopathic cases are attributed to disturbances during the final phase of spermatogenesis, known as spermiogenesis, wherein round spermatids undergo extensive

 doi:10.20944/preprints202511.1008.v1

remodeling to form mature spermatozoa [3]. This process involves a series of highly coordinated morphological changes, such as nuclear elongation, chromatin condensation, acrosome biogenesis, the development of the flagellar axoneme and the periaxonemal structures, the assembly of the mitochondrial sheath in the midpiece, and the extrusion of residual cytoplasm [3]. These changes are critical for motility and fertilization competence [4].

The perinuclear theca (PT), a major cytoskeletal component of the sperm head, consists of various cytosolic and nuclear proteins [5]. The PT is conventionally divided into two functionally distinct regions: the subacrosomal region (SAR), located between the inner acrosomal membrane and the nuclear envelope, and the postacrosomal region (PAR), positioned between the plasma membrane and the nuclear envelope [6,7]. PT-SAR proteins are derived from acrosomal vesicles during acrosome biogenesis, whereas PT-PAR proteins are synthesized in the cytoplasmic lobe and transported across the manchette [8]. Thus, one of the critical functions of PT-SAR proteins is to anchor the developing acrosomes to the sperm nucleus, whereas PT-PAR proteins (e.g. phospholipase C zeta, PLCζ) are primarily involved in the later stages of fertilization process, such as oocyte activation [5–7,9].

ACTRT1 (Actin-Related Protein Testis 1), which is encoded by a single-exon *ACTRT1* gene (OMIM: *300487) located on the X chromosome (Xq25), is a vital component of the PT-SAR-specific actin-related protein complex (ACTRT1-ACTRT2-ACTRT3-ACTL7A-ACTL7B-ACTL9) which anchors developing acrosomes to the nucleus [10]. This complex immunoprecipitates with the inner acrosomal membrane protein SPACA1 and the nuclear envelope proteins PARP11 and SPATA46 [11]. In *Actrt1* knockout mice, the loss of Actrt1 attenuates the interaction between Actl7a and Spaca1 proteins, resulting in severe subfertility characterized by morphologically abnormal sperm heads with detached acrosomes and partial fertilization failure [11]. Similarly, a recent human study identified a 110-kb hemizygous loss-of-function deletion affecting the *ACTRT1* gene in infertile men, presenting with severe oligoteratozoospermia, detached acrosomes, and markedly reduced fertilization rates [12]. As demonstrated by Q. Zhang et al., Actrt1 and Actl7a exhibit a spatiotemporal localization in male germ cells. These proteins are specifically targeted to the SAR in round and elongated spermatids to mediate acrosome-nucleus anchoring during acrosome biogenesis and subsequently relocate to the PAR in mature spermatozoa, positioning them for potential roles in later fertilization stages, such as oocyte activation [11]. Notably, loss or reduced expression and/or abnormal localization of PLCζ has been reported in *ACTRT1*/*ACTL7A*/*ACTL9* mutant patients as well as in *Actrt1*-, *Actl7a*- and *Actl9*-deficient mice [11–24]. Furthermore, disruption of *ACTL7A* or *ACTL9* has been consistently shown to cause acrosome detachment, total fertilization failure, and male infertility in both mice and humans [13–24].

In the present study we identified a novel hemizygous *ACTRT1* gene variant in a patient with severe oligoasthenoteratozoospermia and specific morphological abnormality, characterized by the acrosome detachment from the sperm nucleus, providing new insights into the genetic basis of male infertility.

2. Materials and Methods

2.1. Patient

A 33-year-old male patient was referred to the Research Centre for Medical Genetics for medical genetic counseling and examination due to primary infertility. His clinical history included recurrent severe oligoasthenoteratozoospermia (sOAT), as well as the surgical treatment of right inguinal cryptorchidism via orchiectomy, which was performed in December 2022. Preoperative scrotal ultrasonography revealed significant testicular asymmetry, with a preserved left testicular volume of 16.5 ml and right testicular hypoplasia of 7.64 ml, as well as complete inguinal ectopia. Additionally, a grade I left-sided varicocele was identified. An endocrine evaluation revealed elevated levels of luteinizing hormone (11.50 mIU/mL; reference range: 1.70–8.60), indicating compensated hypogonadism [25]. Normal follicle-stimulating hormone levels (11.30 mIU/mL; reference range:

 doi:10.20944/preprints202511.1008.v1

1.50–12.40) and normal total testosterone levels (6.29 ng/mL; reference range: 2.49–8.36) supported this finding. Standard genetic analysis revealed a normal 46,XY karyotype with no evidence of Y-chromosome microdeletions. Screening for the 22 most common pathogenic *CFTR* variants was negative. Analysis of the polymorphic CAG repeat region of the androgen receptor gene revealed 21 repeats, which is within normal limits. The physical examination was unremarkable, with anthropometric measurements of 178 cm height and 78 kg weight (BMI 24.6 kg/m^2).

The 32-year-old female partner underwent a complete evaluation, that demonstrated normal ovarian reserve parameters and a normal female karyotype (46,XX). The couple underwent an assisted reproductive technology protocol involving intracytoplasmic sperm injection with ejaculated sperm. Ovarian stimulation using a gonadotropin-releasing hormone antagonist protocol resulted in the retrieval of 12 metaphase II oocytes. Despite an optimal ovarian response and sufficient mature oocytes, the cycle was complicated by severe fertilization failure, with only one oocyte demonstrating normal fertilization. According to the standard grading criteria, the resulting embryo had poor morphology (grade 3) and did not implant after transfer. A subsequent ICSI cycle incorporating assisted oocyte activation (AOA) with calcium ionophore is planned due to the fertilization failure observed, in order to overcome the suspected oocyte activation deficiency.

Written informed consent was obtained from all examined individuals. The study was approved by the Ethics Committee of the Research Centre for Medical Genetics (protocol code: №4/3; date of approval: April 19, 2021).

2.2. Standard Semen Examination

Semen samples were collected by masturbation after 3-5 days of sexual abstinence. The analyzed semen parameters included ejaculate volume, viscosity and pH, concentration and total sperm count, motility, vitality and morphology. Sperm vitality (%), motility (%), morphology (%) and sperm count were determined by light microscopy using a Nikon Ci microscope (Nikon, Japan). A standard semen analysis was performed according to the World Health Organization laboratory guideline (WHO, 2010), and the semen parameters were interpreted based on the reference values established in these guideline [26].

2.3. Transmission Electron Microscopy

For the transmission electron microscopy (TEM) analysis, semen samples were obtained from the patient and a control group of 24 fertile, normozoospermic men aged 35 years or younger who had fathered a child within the past 12 months. All control samples exhibited normal semen parameters. After liquefaction, samples from the patient and controls were fixed with a 2.5% glutaraldehyde solution in a 0.1 M cacodylate buffer solution (pH 7.2–7.4). The samples were then treated with 1% osmic acid and embedded in epoxy resin. Ultrathin sections were prepared using a Reichert-Jung Ultracut E ultramicrotome (Vienna, Austria) and mounted on copper grids covered with Formvar film. The sections were then contrasted using a 1% aqueous solution of uranyl acetate and a lead citrate solution. The preparations were examined at 80 kV using a JEM-1011 transmission electron microscope (JEOL, Akishima, Japan), which was equipped with an Orius SC1000 W camera (Gatan Inc., Pleasanton, CA, USA). Results for each parameter are expressed as percentages.

2.4. Isolation of Genomic DNA

Genomic DNA of the proband and his mother was extracted from peripheral blood leukocytes using a standard Wizard® Genomic DNA Purification Kit (Promega, USA) according to the manufacturer's protocol.

2.5. Whole Exome Sequencing

Whole exome sequencing (WES) was performed on the proband's DNA sample. Libraries were prepared from fragmented genomic DNA using the KAPA Hyper Prep Kit (Roche, Switzerland), and

 doi:10.20944/preprints202511.1008.v1

target enrichment was carried out using KAPA HyperExome probes (Roche, Switzerland). Paired-end sequencing (2 × 150 bp) was conducted on an Illumina NextSeq 500 platform.

The resulting raw data were aligned to the human reference genome (GRCh37/hg19) using NGSData software. Sequencing achieved a mean coverage of 78x, with 97% of target regions covered at least 10x. Variant calling and annotation were performed according to the standard HGVS nomenclature. The identified variant was visualized using the Integrative Genomics Viewer v.2.17.4 (IGV), and its pathogenicity was assessed in accordance with the guidelines of the American College of Medical Genetics and Genomics (ACMG) [27].

2.6. Sanger Sequencing

To validate the variant identified by WES, exon 1 of the *ACTRT1* gene was amplified from genomic DNA using PCR with the following primers, synthesized by Eurogen (Moscow, Russia): forward 5′ AGAGGTCATGATGGATGCACCA, reverse 5′ TTGGGGATGAGCTGTACCAAGT. PCR was performed in 25 µl PCR reactions containing 1×PCR buffer, 2 mM $MgCl_2$, 0.2 mM of each dNTP, 0.5 mM of each primer, 0,3 U of Taq DNA polymerase (Syntol, Russia), and 1 µL of genomic DNA. Cycling was performed using a GeneAmp PCR System 9700 Thermal Cycler (Applied Biosystems) with the following cycle program: Initial denaturation at 95°C for 2 minutes followed by 35 cycles of 95°C for 30 seconds, 64°C for 30 seconds and 72°C for 30 seconds, followed by a final extension of 5 minutes at 72°C. Five µL of the PCR products were visualized on 2% agarose gels using ethidium bromide staining and UV light transillumination. Amplicons were purified using an Exonuclease I 20 U/µL/FastAP Thermosensitive Alkaline Phosphatase 1 U/µL (Thermo Fisher Scientific, USA) mixture. Purified PCR products were sequenced using the BigDye Terminator Kit v3.1 (Thermo Fisher Scientific, USA) and Applied Biosystems 3500 DNA Analyzer (Thermo Fisher Scientific, USA) according to the manufacturer's protocol. The result of the sequences data was visualized by Chromas software v.2.6.6 (Technelysium, Australia).

2.7. In Silico Pathogenicity Prediction and Structural Analysis of Detected Variant

The potential pathogenicity of the identified missense variant was assessed using a comprehensive suite of bioinformatics tools, including: SIFT, SIFT4G, PROVEAN, MutationTaster, LRT, FATHMM, DANN, MetaLR, MetaSVM, M-CAP, MutationAssessor, MutPred, MVP, PrimateAI, EIGEN, EIGEN-PC and DEOGEN2.

The evolutionary conservation of the affected amino acid position was analyzed using the UCSC Genome Browser (https://genome.ucsc.edu/, accessed on 20 June 2024). The impact of the amino acid substitution on protein structure was visualized and analyzed using the Project HOPE web portal (https://www3.cmbi.umcn.nl/hope/, accessed on 17 June 2024) [28].

3. Results

3.1. Semen Analysis

Repeated semen analyses revealed low sperm concentrations ranging from 0.2 to 2.8 (1.1 ± 1.2) million per milliliter and correspondingly reduced total sperm counts of 3.2 ± 3.5 × 10^6 per ejaculate in the four examined samples (Table S1). The sperm motility parameters decreased dramatically. Progressive motility (PR) was severely low at 0–9% (5.3 ± 3.8%), and total motility (PR + NP) was below the reference range of ≥40% in two samples (26% and 37%). However, it was normal in the last two samples (42% and 51%). Sperm vitality exhibited considerable variability (71.5 ± 21.4%), ranging from severely compromised to normal (45–91%). Severe teratozoospermia was also consistently observed in all examined samples (99-100% abnormal morphology), with only 0.5% ± 0.6% of gametes being morphologically normal. Head defects were the predominant morphological abnormality, present in 65–75% (70.0 ± 4.5%) of gametes. The volume and pH of the ejaculate were within the normal range (2.9 ± 0.4 mL and 7.6 ± 0.1, respectively). The leukocyte concentration was within the

 doi:10.20944/preprints202511.1008.v1

normal reference range (0.16 ± 0.11 million/mL), thereby excluding an inflammatory etiology (Table S1).

3.2. Transmission Electron Microscopy

TEM revealed significant ultrastructural abnormalities in the patient's spermatozoa (Figures 1C, 1D, 1E, and 1E1), but not in the control group (Figures 1A and 1B, Table S2).

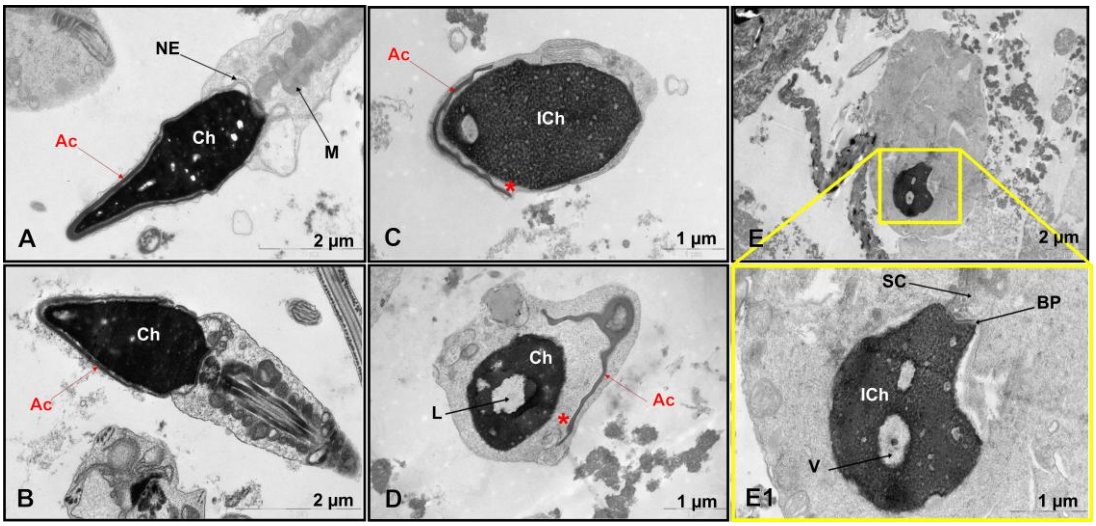

Figure 1. Ultrastructural sperm defects in a patient with severe oligoteratozoospermia. (A, B) Spermatozoa from a fertile control donor demonstrate normal ultrastructure, with acrosomes tightly apposed to the nucleus. (C, D, E, E1) Spermatozoa from the patient showing characteristic pathological features, including: acrosomal hypoplasia and detachment from the nuclear envelope (C, D), acrosomal aplasia (E,E1), and impaired chromatin condensation (C,E1). Abbreviations: Ac: acrosome (red arrows); Ch: chromatin; NE: nuclear envelope; M: mitochondria; Ich: immature chromatin; L: lacuna; *: the enlarged space between the acrosome and the nucleus; V: vacuole; BP: basal plate of the sperm neck; SC: segmented columns of the connecting piece of the sperm flagellum.

A comparative ultrastructural analysis of sperm morphology revealed an absence of spermatozoa with intact heads in the patient (0%), in contrast to the control group, in which such cells constituted 5.4 ± 1.7% (range 4-9%). Although the incidence of acrosome hypoplasia in the patient (42%) was within the normal reference range (46.0 ± 11.7%, range 7-61%), other critical parameters showed significant deviations. Notably, the proportion of spermatozoa with impaired chromatin condensation was markedly higher at 54% versus 17.0 ± 8.3% (range 7-29%) in the control group. Similarly, spermatozoa with excessive residual cytoplasm accounted for 31% of the patient's sample, compared to 6.2 ± 3.9% (range 1-13%) in the control group. The percentage of spermatozoa with an enlarged subacrosomal space was 49%, compared to a control value of 5.3 ± 3.4% (range 1-11%). Additionally, the incidence of flagellar axoneme abnormalities was substantially higher in the patient (31%) than in the control group (9.7 ± 7.6%, range 1-30%).

The most pronounced pathological features were the complete absence of normally formed sperm heads, characterized by detachment of the inner acrosomal membrane from the sperm nucleus, severe chromatin condensation defects, excessive cytoplasmic retention, and a high percentage of enlarged subacrosomal spaces (Figures 1C, 1D, 1E, and 1E1).

Because of the high prevalence of specific ultrastructural defects revealed by the TEM results, the patient was referred for WES to identify an underlying genetic etiology.

3.3. Molecular Genetic, Segregation and Bioinformatic Study Results

Initial variant filtering and annotation focused on known genes associated with male infertility revealed no pathogenic, likely pathogenic, or variants of unknown clinical significance in established

 doi:10.20944/preprints202511.1008.v1

oligoteratozoospermia-related genes. Subsequent analysis identified a novel hemizygous missense variant in the *ACTRT1* gene (NM_138289.4), located on the X chromosome (locus Xq25). This variant is characterized by a c.821G>C substitution that results in an amino acid change from glycine to alanine at position 274 (Figure 2). A comprehensive review of the Online Mendelian Inheritance in Man (OMIM) database revealed no established associations between the *ACTR1* gene and male infertility. This suggests that this finding may represent a novel genotype-phenotype correlation. The identified nucleotide sequence variant is not registered in the control sample Genome Aggregation Database (gnomAD v2.1.1) (http://gnomad.broadinstitute.org/).

Evolutionary conservation analysis revealed that the affected glycine residue at position 274 is highly conserved among vertebrate species, indicating significant structural or functional constraints at this site of the ACTRT1 protein (Figure 2A).

Sanger sequencing was performed for the proband and his mother, and the results confirmed an X-linked recessive inheritance pattern. The variant was hemizygous in the proband and heterozygous in his asymptomatic mother (Figure 2C). This pattern of inheritance is consistent with Mendelian inheritance for X-chromosomal disorders and suggests that the variant may be pathogenic in a hemizygous state for male patients.

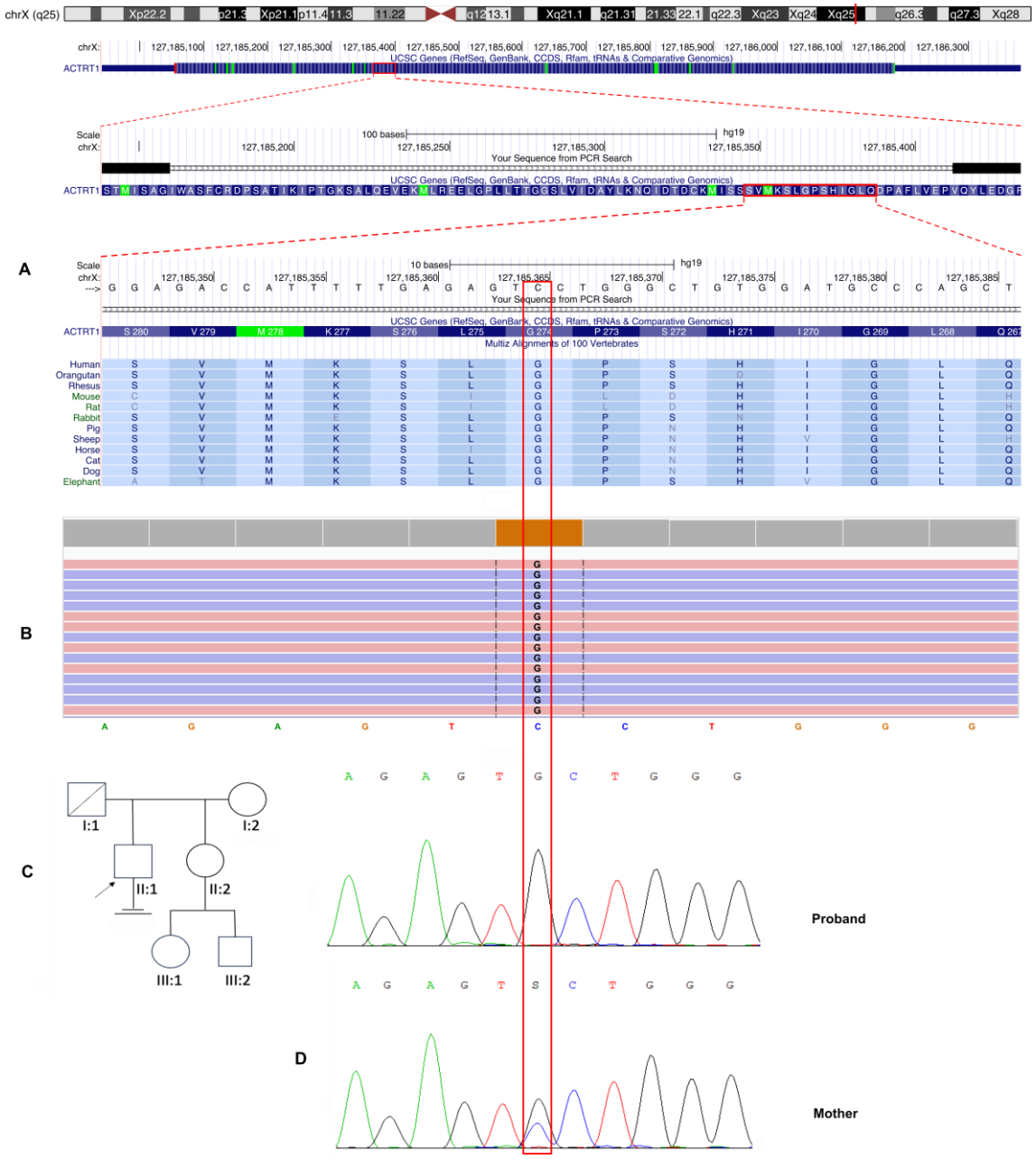

 doi:10.20944/preprints202511.1008.v1

Figure 2. Identification and validation of a novel *ACTRT1* gene variant. (A) Schematic localization of the X-linked *ACTRT1* gene and evolutionary conservation analysis. The gene structure comprises a single exon. The identified c.821G>C, p.(Gly274Ala) missense variant is indicated at the genomic coordinate chrX:127185365. Multiple sequence alignment across diverse species demonstrates that the glycine residue at position 274 is completely evolutionarily conserved (indicated by a red frame), highlighting its putative structural and functional importance. (B) Visualization of the hemizygous chrX:127185365C>G substitution in the *ACTRT1* gene using Integrative Genomics Viewer (IGV v2.17.4) software. (C) Pedigree of a patient with sOAT. The proband is indicated by an arrow. Circles represent females, and squares represent males. Deceased family members are denoted by a diagonal slash. A vertical line with two horizontal crossbars marks the infertile couple. (D) Sanger sequencing of a proband and his mother. Sanger sequencing confirmed the c.821G>C, p.(Gly274Ala) substitution in a hemizygous state in the proband and in a heterozygous state in the maternal carrier. The substitution site is highlighted with a red frame.

The variant c.821G>C is considered likely pathogenic by pathogenicity prediction algorithms for missense variants (SIFT, SIFT4G, BLOSUM, DANN, FATHMM, PrimateAI, MetaLR, MetaSVM, DEOGEN2, EIGEN, EIGEN PC, M-CAP, Mutation assessor, MutPred, MVP, PROVEAN, LRT, MutationTaster).

We have also created a 3D model of the mutant ACTRT1 protein and compared it with the normal protein using the Project HOPE3D tool (Figure 3).

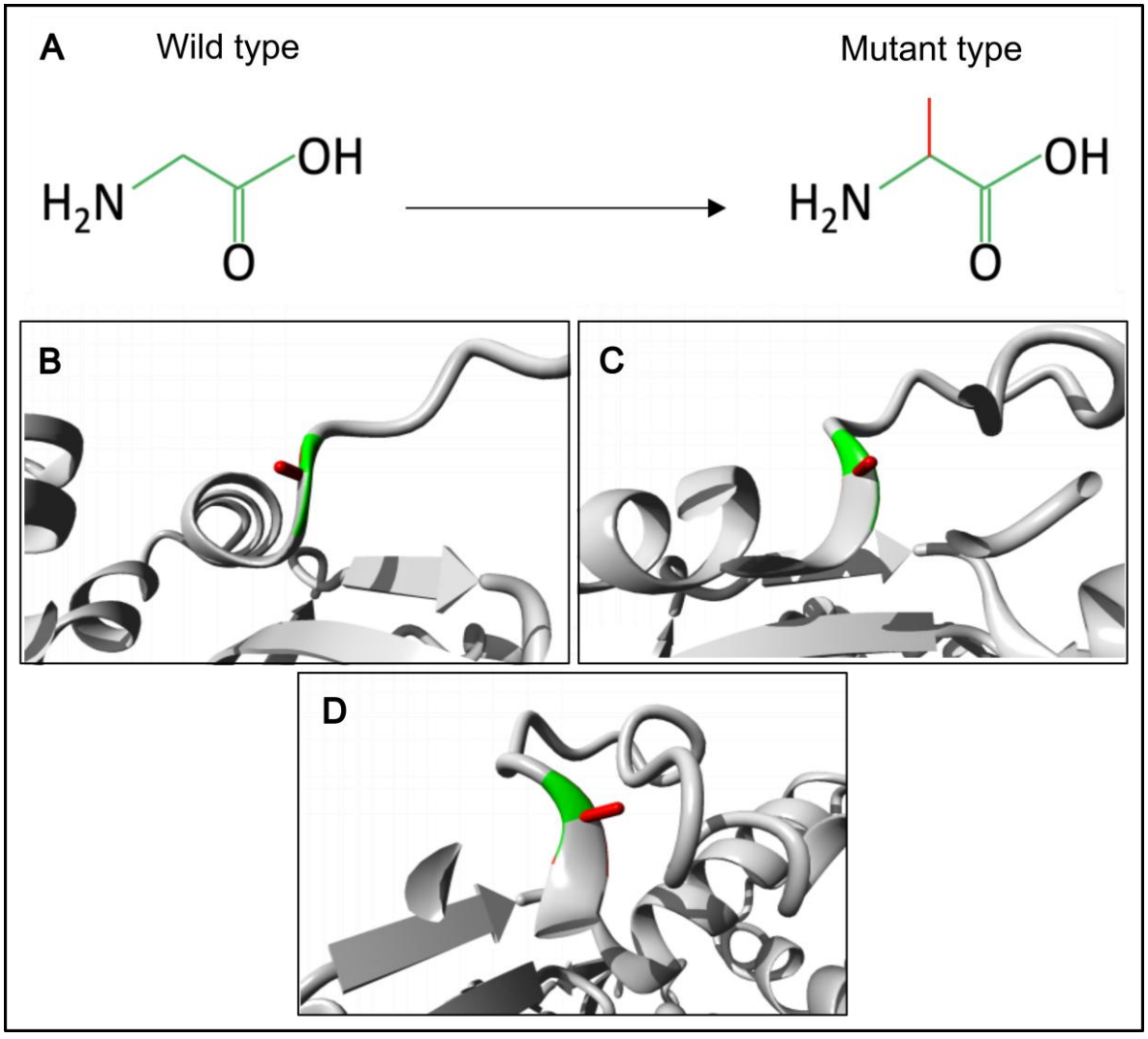

Figure 3. 3D model of normal and mutant ACTRT1 protein structure. (A) A schematic comparison of the wild-type glycine residue (left) and the mutant alanine residue (right), with the common backbone shown in green

 doi:10.20944/preprints202511.1008.v1

and the unique side chains shown in red. (B–D) Close-up views of the substitution site from different angles, with the protein backbone shown in gray and the wild-type and mutant side chains shown in green and red, respectively.

The p.(Gly274Ala) substitution in the ACTRT1 introduces significant steric constraints due to the substantial difference in side-chain volume between glycine and alanine. The larger alanine residue cannot be accommodated within the core structure, leading to unfavorable torsion angles and steric clashes. The unique conformational flexibility of glycine is essential at this position, as it is the only residue capable of adopting the required backbone conformation without distortion. Substitution with alanine is predicted to disrupt the local protein architecture, an effect that would likely propagate to destabilize the tertiary structure of ACTRT1 and compromise its biological function. Therefore, glycine is exclusively required to maintain the native protein fold at this position.

Finally, the identified variant chrX:127185365G>C; NM_138289.3: c.821G>C, p.(Gly274Ala) in the *ACTRT1* gene was classified as a variant of uncertain clinical significance (VoUS) according to the ACMG guidelines (PM2, PP3).

4. Discussion

The *ACTRT1* gene encodes the actin-related protein T1, a critical structural component of a testis-specific ARP complex (ACTRT1-ACTRT2-ACTL7A-ACTL7B-ACTL9) within the PT, which is indispensable for anchoring the acrosome to the sperm nucleus and fertilization [11]. Despite its testis-restricted expression profile, the previously established OMIM phenotype associated with *ACTRT1* gene was Bazex-Dupré-Christol syndrome (BDCS; OMIM: 301845), an X-linked dominant genodermatosis characterized by follicular atrophoderma, congenital hypotrichosis, and early-onset multiple basal cell carcinomas [29,30]. However, recent evidence has definitively refuted this association. Liu et al. (2022) demonstrated that BDCS is actually caused by small intergenic tandem duplications at Xq26.1, leading to dysregulation of the *ARHGAP36* gene [31]. Importantly, no rare coding variants in the *ACTRT1* gene were identified in 7 of 8 BDCS families. Furthermore, immunofluorescence studies revealed the absence of *ACTRT1* expression in relevant hair follicle compartments [31]. Therefore, *ACTRT1* has been excluded as a causative gene for BDCS. Its actual phenotypic consequences remain to be fully elucidated; however, its testis-specific expression and structural role suggest potential involvement in male reproductive function, which requires further validation.

The initial link between *ACTRT1* and male infertility was established in a large-scale sequencing study. S. Chen et al. (2020) conducted a whole exome sequencing analysis of 314 Chinese men with non-obstructive azoospermia (NOA) and severe oligozoospermia and identified *ACTRT1* as one of 20 novel candidate genes for male infertility [32]. Among the patients in their cohort, two patients with NOA were found to have hemizygous variants in the *ACTRT1* gene [32]. Notably, a meiotic arrest phenotype was revealed by testicular histopathology in both patients.

Subsequently, Y. Sha et al. (2021) proposed a more specific yet controversial association [33]. They identified two unrelated individuals with hemizygous missense variants in *ACTRT1* in a cohort of 34 infertile men with acephalic spermatozoa syndrome (ASS). The patients presented with asthenoteratozoospermia, characterized predominantly by acephalic sperm. Immunofluorescence staining revealed displaced and diffuse *ACTRT1* expression in the patients' sperm. To validate their findings, the researchers generated an *Actrt1*-knockout mouse model using CRISPR/Cas9 and reported that approximately 60% of the sperm were headless, with TEM revealing significant defects in the head-tail coupling apparatus (HTCA). Based on this, they proposed *ACTRT1* as a gene associated with ASS. Following artificial insemination with optimized sperm, both patients and their partners achieved successful pregnancy and delivery.

However, this conclusion was challenged by a series of studies from another research group. X. Zhang et al. (2022) reanalyzed the role of *ACTRT1*, identifying it as a candidate gene in patients with syndromic teratozoospermia characterized not by headless sperm, but specifically by the detachment

 doi:10.20944/preprints202511.1008.v1

of the acrosome from the sperm nucleus [11]. This refined phenotype was strongly supported by functional mouse model data. Their *Actrt1*-knockout mice were severely subfertile, exhibiting deformed sperm heads and a high proportion of sperm with detached acrosomes, as confirmed by TEM. These results allowed to reveal that ACTRT1 interacts with ACTRT2, ACTL7A, and ACTL9 to form a sperm-specific PT-ARP complex, which anchors the developing acrosome to the nucleus by connecting the inner acrosomal membrane protein SPACA1 with nuclear envelope proteins such as PARP11 and SPATA46. Importantly, their *Actrt1-KO* mice did not exhibit the headless sperm phenotype reported by Sha et al., despite using a similar knockout strategy. The authors argued that there was no evidence that ACTRT1 regulates the HTCA and deemed the evidence linking it to ASS insufficient.

The human relevance of this acrosome detachment phenotype was conclusively demonstrated by Q. Zhang et al. (2024) [12]. They reported two infertile Chinese men with a ~110 kb X-chromosomal microdeletion encompassing the entire *ACTRT1* gene. Semen analysis revealed sOT, and TEM confirmed sperm head deformation due to acrosome detachment, perfectly mirroring the mouse model. The deletion was inherited from the patients' mothers, consistent with X-linked recessive inheritance. Western blot and immunostaining of patient sperm showed that ACTRT1 deficiency led to downregulated expression and ectopic distribution of ACTL7A and PLCζ, key proteins for oocyte activation, explaining the observed fertilization failure. The authors successfully overcame this challenge by using the ICSI procedure combined with artificial oocyte activation (AOA) on one patient.

In the study by H. Zhou et al. (2024), a patient with oligoasthenoteratozoospermia (OAT) was found to carry a hemizygous missense mutation in the *ACTRT1* gene [34].

The clinical and genetic features of all male patients with reported *ACTRT1* variants are summarized in Table 1.

Table 1. Clinical and genetics characteristic of patients with the *ACTRT1* (NM_138289.4) gene variants.

Patient	Gene variant	Phenotype/additional data	References
NOA54	c.662A>G, p.(Tyr221Cys)	NOA with meiotic arrest. Normal male karyotype (46,XY) without AZF microdeletions; normal endocrine profile (FSH, LH, total testosterone) and testis volume	S. Chen et al., 2020 [32]
NOA281	c.431C>T, p.(Ala144Val)		
F018	c.95G>A, p.(Arg32His)	Asthenoteratozoospermia, ASS	Y. Sha et al., 2021 [33]
F034	c.662A>G, p.(Tyr221Cys)		
L053	110-kb deletion	sOT; acrosome detachment, fertilization failure	Q. Zhang et al., 2024 [12]
L116			
M1555	c.169G>A, p.(Val157Met)	OAT. Normal male karyotype (46,XY), no AZF microdeletions	H. Zhou et al., 2024 [34]
Present	c.821G>C, p.(Gly274Ala)	sOAT; acrosome detachment, fertilization failure	

NOA – non-obstructive azoospermia; FSH – follicle stimulating hormone; LH – luteinizing hormone; ASS – acephalic sperm syndrome; sOT – severe oligoteratozoospermia; sOAT – severe oligoteratozoospermia.

In our patient, a history of right inguinal cryptorchidism requiring orchiectomy could certainly be a contributing factor to his severe oligozoospermia. However, the specific ultrastructural defects revealed by TEM—particularly the abnormal sperm head morphology characterized by detachment of the inner acrosomal membrane from the nucleus—are highly consistent with the phenotypes observed in both *Actrt1*-knockout mouse models and in patients with complete *ACTRT1* deletion. However, a comprehensive comparison with other reported *ACTRT1* variant cases is limited. For patients with non-obstructive azoospermia or severe oligoasthenoteratozoospermia TEM analysis was precluded due to the absence or critically low number of spermatozoa in the ejaculate. This

 doi:10.20944/preprints202511.1008.v1

makes it impossible to determine whether acrosomal detachment is a universal feature. Furthermore, data on the percentage of spermatozoa with immature chromatin or flagellar axonemal abnormalities are unavailable in other patients with identified *ACTRT1* variants. In our case, the significant finding is the high proportion (54%) of spermatozoa with non-condensed chromatin, as defective chromatin compaction is a well-established factor that can impair paternal DNA integrity and potentially lead to failures in embryonic cleavage, division, and early development. These findings suggest that the phenotypic spectrum of *ACTRT1*-related infertility may extend beyond acrosomal defects to include nuclear and abnormalities, which could collectively contribute to variable clinical and ART outcomes observed among patients.

These findings provide strong circumstantial evidence linking this specific genetic variant to the observed spermatological profile, the characteristic ultrastructural defects, and the clinical outcome of failed fertilization. However, direct functional studies are required to definitively characterize the pathogenic impact of the p.(Gly274Ala) substitution on the ACTRT1 protein.

As demonstrated by the literature, male patients with hemizygous variants in the *ACTRT1* gene exhibit a remarkably heterogeneous clinical spectrum, ranging from asthenoteratozoospermia and acephalic spermatozoa syndrome to severe oligozoospermia and non-obstructive azoospermia with meiotic arrest. This significant phenotypic variability highlights the importance of collecting and reporting detailed clinical cases that integrate comprehensive semen analysis, TEM, and genetic data. These efforts are essential for delineating precise genotype-phenotype correlations and understanding the full pathogenic potential of *ACTRT1* gene variants in human male infertility.

5. Conclusions

This study provides a comprehensive clinical and genetic characterization of a novel *ACTRT1* gene variant in a patient with severe oligoteratozoospermia and fertilization failure. The results contribute to the growing evidence linking *ACTRT1* deficiency to specific head defects with acrosomal detachment and other sperm abnormalities. These findings support the inclusion of *ACTRT1* in genetic screening panels for azoospermic or severe oligoteratozoospermic patients, as well as the use of transmission electron microscopy for teratozoospermic patients with fertilization failure, and highlight the need for additional functional studies to establish definitive genotype-phenotype correlations.

Supplementary Materials: The following supporting information can be downloaded at the website of this paper posted on Preprints.org.

Author Contributions: Conceptualization, O.S. and V.C.; methodology, O.S.; validation, S.Kh. and T.C.; formal analysis, S.Kh.; investigation, O.S., E.B., and S.B.; resources, O.S. and S.B.; data curation, O.S. and S.Kh.; writing—original draft preparation, O.S. and V.C.; writing—review and editing, S.Kh., S.B., E.B., T.C.; visualization, V.C.; supervision, O.S. and V.C.; project administration, V.C. All authors have read and agreed to the published version of the manuscript.

Funding: This research was funded by the Russian Science Foundation (project No. 25-25-00577, https://rscf.ru/project/25-25-00577/).

Institutional Review Board Statement: The study was conducted in accordance with the Declaration of Helsinki, and approved by the Institutional Review Board (or Ethics Committee) of Research Centre for Medical Genetics (protocol code: №4/3; date of approval: April 19, 2021).

Informed Consent Statement: Informed consent was obtained from all subjects involved in the study, and written informed consent has been obtained from the patients to publish this paper.

Data Availability Statement: The original contributions presented in the study are included in the article. Further inquiries can be directed to the corresponding author.

 doi:10.20944/preprints202511.1008.v1

Acknowledgments: Ultrastructural studies supported by the State Assignment of the Lomonosov Moscow State University (No. 21870-PV-DCH).

Conflicts of Interest: The authors declare no conflicts of interest.

Abbreviations

The following abbreviations are used in this manuscript:

AZF	AZoospermia Factor
CFTR	Cystic Fibrosis Transmembrane conductance Regulator
PT	Perinuclear Theca
SAR	SubAcrosomal Region
PAR	PostAcrosomal Region
FSH	Follicle Stimulating Hormone
LH	Luteinizing Hormone
WHO	World Health Organization
TEM	Transmission Electron Microscopy
WES	Whole Exome Sequencing
IGV	Integrative Genome Viewer
ACMG	American College of Medical Genetics and Genomics
sOT	severe OligoTeratozoospermia
sOAT	Severe OligoAsthenoTeratozoospermia
BMI	Body Mass Index
OMIM	Online Mendelian Inheritance in Man
gnomAD	genome Aggregation Database
PLCζ	Phospholipase C Zeta
ASS	Acephalic Sperm Syndrome
HTCA	Head-Tail Coupling Apparatus
BDS	Bazex-Dupré-Christol syndrome
AOA	Assisted Oocyte Activation

References

1. Krausz, C. Male Infertility: Pathogenesis and Clinical Diagnosis. *Best Pract Res Clin Endocrinol Metab* **2011**, *25*, 271–285, doi:10.1016/j.beem.2010.08.006.
2. Houston, B.J.; Riera-Escamilla, A.; Wyrwoll, M.J.; Salas-Huetos, A.; Xavier, M.J.; Nagirnaja, L.; Friedrich, C.; Conrad, D.F.; Aston, K.I.; Krausz, C.; et al. A Systematic Review of the Validated Monogenic Causes of Human Male Infertility: 2020 Update and a Discussion of Emerging Gene–Disease Relationships. *Hum Reprod Update* **2021**, *28*, 15–29, doi:10.1093/humupd/dmab030.
3. Miyata, H.; Shimada, K.; Kaneda, Y.; Ikawa, M. Development of Functional Spermatozoa in Mammalian Spermiogenesis. *Development* **2024**, *151*, doi:10.1242/dev.202838.
4. Du, L.; Chen, W.; Cheng, Z.; Wu, S.; He, J.; Han, L.; He, Z.; Qin, W. Novel Gene Regulation in Normal and Abnormal Spermatogenesis. *Cells* **2021**, *10*, 666, doi:10.3390/cells10030666.
5. Oko, R.; Sutovsky, P. Biogenesis of Sperm Perinuclear Theca and Its Role in Sperm Functional Competence and Fertilization. *J Reprod Immunol* **2009**, *83*, 2–7, doi:10.1016/j.jri.2009.05.008.
6. Oko, R. Developmental Expression and Possible Role of Perinuclear Theca Proteins in Mammalian Spermatozoa. *Reprod Fertil Dev* **1995**, *7*, 777, doi:10.1071/RD9950777.
7. Longo, F.J.; Cook, S. Formation of the Perinuclear Theca in Spermatozoa of Diverse Mammalian Species: Relationship of the Manchette and Multiple Band Polypeptides. *Mol Reprod Dev* **1991**, *28*, 380–393, doi:10.1002/mrd.1080280411.
8. Schneider, S.; Kovacevic, A.; Mayer, M.; Dicke, A.-K.; Arévalo, L.; Koser, S.A.; Hansen, J.N.; Young, S.; Brenker, C.; Kliesch, S.; et al. Cylicins Are a Structural Component of the Sperm Calyx Being Indispensable for Male Fertility in Mice and Human. *Elife* **2023**, *12*, doi:10.7554/eLife.86100.
9. Oko, R.; Maravei, D. Protein Composition of the Perinuclear Theca of Bull Spermatozoa1. *Biol Reprod* **1994**, *50*, 1000–1014, doi:10.1095/biolreprod50.5.1000.

 doi:10.20944/preprints202511.1008.v1

10. Heid, H.W.; Figge, U.; Winter, S.; Kuhn, C.; Zimbelmann, R.; Franke, W.W. Novel Actin-Related Proteins Arp-T1 and Arp-T2 as Components of the Cytoskeletal Calyx of the Mammalian Sperm Head. *Exp Cell Res* **2002**, *279*, 177–187, doi:10.1006/excr.2002.5603.
11. Zhang, X.-Z.; Wei, L.-L.; Zhang, X.-H.; Jin, H.-J.; Chen, S.-R. Loss of Perinuclear Theca ACTRT1 Causes Acrosome Detachment and Severe Male Subfertility in Mice. *Development* **2022**, *149*, doi:10.1242/dev.200489.
12. Zhang, Q.; Jin, H.; Long, S.; Tang, X.; Li, J.; Liu, W.; Han, W.; Liao, H.; Fu, T.; Huang, G.; et al. Deletion of ACTRT1 Is Associated with Male Infertility as Sperm Acrosomal Ultrastructural Defects and Fertilization Failure in Human. *Hum Reprod* **2024**, *39*, 880–891, doi:10.1093/humrep/deae031.
13. Zhou, X.; Liu, Z.; Jia, W.; Hou, M.; Zhang, X. Actl7a Deficiency in Mice Leads to Male Infertility and Fertilization Failure. *Biochem Biophys Res Commun* **2022**, *623*, 154–161, doi:10.1016/j.bbrc.2022.07.065.
14. Zhou, J.; Zhang, B.; Zeb, A.; Ma, A.; Chen, J.; Zhao, D.; Rahim, F.; Khan, R.; Zhang, H.; Zhang, Y.; et al. A Recessive ACTL7A Founder Variant Leads to Male Infertility Due to Acrosome Detachment in Pakistani Pashtuns. *Clin Genet* **2023**, *104*, 564–570, doi:10.1111/cge.14383.
15. Dai, J.; Chen, Y.; Li, Q.; Zhang, T.; Zhou, Q.; Gong, F.; Lu, G.; Zheng, W.; Lin, G. Pathogenic Variant in ACTL7A Causes Severe Teratozoospermia Characterized by Bubble-Shaped Acrosomes and Male Infertility. *Mol Hum Reprod* **2022**, *28*, doi:10.1093/molehr/gaac028.
16. Zhou, X.; Xi, Q.; Jia, W.; Li, Z.; Liu, Z.; Luo, G.; Xing, C.; Zhang, D.; Hou, M.; Liu, H.; et al. A Novel Homozygous Mutation in ACTL7A Leads to Male Infertility. *Molecular Genetics and Genomics* **2023**, *298*, 353–360, doi:10.1007/s00438-022-01985-0.
17. Zhao, S.; Cui, Y.; Guo, S.; Liu, B.; Bian, Y.; Zhao, S.; Chen, Z.; Zhao, H. Novel Variants in ACTL7A and PLCZ1 Are Associated with Male Infertility and Total Fertilization Failure. *Clin Genet* **2023**, *103*, 603–608, doi:10.1111/cge.14293.
18. Xin, A.; Qu, R.; Chen, G.; Zhang, L.; Chen, J.; Tao, C.; Fu, J.; Tang, J.; Ru, Y.; Chen, Y.; et al. Disruption in ACTL7A Causes Acrosomal Ultrastructural Defects in Human and Mouse Sperm as a Novel Male Factor Inducing Early Embryonic Arrest. *Sci Adv* **2020**, *6*, eaaz4796, doi:10.1126/sciadv.aaz4796.
19. Wang, J.; Zhang, J.; Sun, X.; Lin, Y.; Cai, L.; Cui, Y.; Liu, J.; Liu, M.; Yang, X. Novel Bi-Allelic Variants in ACTL7A Are Associated with Male Infertility and Total Fertilization Failure. *Hum Reprod* **2021**, *36*, 3161–3169, doi:10.1093/humrep/deab228.
20. Wang, M.; Zhou, J.; Long, R.; Jin, H.; Gao, L.; Zhu, L.; Jin, L. Novel ACTL7A Variants in Males Lead to Fertilization Failure and Male Infertility. *Andrology* **2025**, *13*, 1117–1126, doi:10.1111/andr.13553.
21. Li, Q.; Huang, Y.; Zhang, S.; Gong, F.; Lu, G.; Lin, G.; Dai, J. Homozygous ACTL9 Mutations Cause Irregular Mitochondrial Sheath Arrangement and Abnormal Flagellum Assembly in Spermatozoa and Male Infertility. *J Assist Reprod Genet* **2024**, *41*, 2271–2278, doi:10.1007/s10815-024-03171-0.
22. Xue, Y.; Cheng, X.; Xiong, Y.; Li, K. Gene Mutations Associated with Fertilization Failure after in Vitro Fertilization/Intracytoplasmic Sperm Injection. *Front Endocrinol (Lausanne)* **2022**, *13*, doi:10.3389/fendo.2022.1086883.
23. Dai, J.; Zhang, T.; Guo, J.; Zhou, Q.; Gu, Y.; Zhang, J.; Hu, L.; Zong, Y.; Song, J.; Zhang, S.; et al. Homozygous Pathogenic Variants in ACTL9 Cause Fertilization Failure and Male Infertility in Humans and Mice. *Am J Hum Genet* **2021**, *108*, 469–481, doi:10.1016/j.ajhg.2021.02.004.
24. Sinaei, R.; Eslami, M.; Dadfar, M.; Saberi, A. Identification of a New Mutation in the ACTL9 Gene in Men with Unexplained Infertility. *Mol Genet Genomic Med* **2024**, *12*, e2448, doi:10.1002/mgg3.2448.
25. Tajar, A.; Forti, G.; O'Neill, T.W.; Lee, D.M.; Silman, A.J.; Finn, J.D.; Bartfai, G.; Boonen, S.; Casanueva, F.F.; Giwercman, A.; et al. Characteristics of Secondary, Primary, and Compensated Hypogonadism in Aging Men: Evidence from the European Male Ageing Study. *J Clin Endocrinol Metab* **2010**, *95*, 1810–1818, doi:10.1210/jc.2009-1796.
26. World Health Organization. WHO Laboratory Manual for the Examination and Processing of Human Semen. **2010**, 271.
27. Richards, S.; Aziz, N.; Bale, S.; Bick, D.; Das, S.; Gastier-Foster, J.; Grody, W.W.; Hegde, M.; Lyon, E.; Spector, E.; et al. Standards and Guidelines for the Interpretation of Sequence Variants: A Joint Consensus Recommendation of the American College of Medical Genetics and Genomics and the Association for Molecular Pathology. *Genetics in Medicine* **2015**, *17*, 405–424, doi:10.1038/gim.2015.30.

28. Venselaar, H.; Te Beek, T.A.H.; Kuipers, R.K.P.; Hekkelman, M.L.; Vriend, G. Protein Structure Analysis of Mutations Causing Inheritable Diseases. An e-Science Approach with Life Scientist Friendly Interfaces. *BMC Bioinformatics* **2010**, *11*, 548, doi:10.1186/1471-2105-11-548.
29. AlSabbagh, M.M.; Baqi, M.A. Bazex-Dupré-Christol Syndrome: Review of Clinical and Molecular Aspects. *Int J Dermatol* **2018**, *57*, 1102–1106, doi:10.1111/ijd.14065.
30. Park, H.-S.; Papanastasi, E.; Blanchard, G.; Chiticariu, E.; Bachmann, D.; Plomann, M.; Morice-Picard, F.; Vabres, P.; Smahi, A.; Huber, M.; et al. ARP-T1-Associated Bazex-Dupré-Christol Syndrome Is an Inherited Basal Cell Cancer with Ciliary Defects Characteristic of Ciliopathies. *Commun Biol* **2021**, *4*, 544, doi:10.1038/s42003-021-02054-9.
31. Liu, Y.; Banka, S.; Huang, Y.; Hardman-Smart, J.; Pye, D.; Torrelo, A.; Beaman, G.M.; Kazanietz, M.G.; Baker, M.J.; Ferrazzano, C.; et al. Germline Intergenic Duplications at Xq26.1 Underlie Bazex–Dupré–Christol Basal Cell Carcinoma Susceptibility Syndrome. *British Journal of Dermatology* **2022**, *187*, 948–961, doi:10.1111/bjd.21842.
32. Chen, S.; Wang, G.; Zheng, X.; Ge, S.; Dai, Y.; Ping, P.; Chen, X.; Liu, G.; Zhang, J.; Yang, Y.; et al. Whole-Exome Sequencing of a Large Chinese Azoospermia and Severe Oligospermia Cohort Identifies Novel Infertility Causative Variants and Genes. *Hum Mol Genet* **2020**, *29*, 2451–2459, doi:10.1093/hmg/ddaa101.
33. Sha, Y.; Liu, W.; Li, L.; Serafimovski, M.; Isachenko, V.; Li, Y.; Chen, J.; Zhao, B.; Wang, Y.; Wei, X. Pathogenic Variants in ACTRT1 Cause Acephalic Spermatozoa Syndrome. *Front Cell Dev Biol* **2021**, *9*, 676246, doi:10.3389/fcell.2021.676246.
34. Zhou, H.; Yin, Z.; Ni, B.; Lin, J.; Luo, S.; Xie, W. Whole Exome Sequencing Analysis of 167 Men with Primary Infertility. *BMC Med Genomics* **2024**, *17*, 230, doi:10.1186/s12920-024-02005-3.